Published in final edited form as:
Brain Res. 2012 November 27; 1486C: 121–130. doi:10.1016/j.brainres.2012.09.039.

Simvastatin Attenuates Axonal Injury after Experimental Traumatic Brain Injury and Promotes Neurite Outgrowth of Primary Cortical Neurons

Hongtao Wu, MD[1], **Asim Mahmood, MD**[1], **Changsheng Qu, MD**[1], **Ye Xiong, MD, PhD**[1], and **Michael Chopp, PhD**[2,3]

[1]Department of Neurosurgery, Henry Ford Hospital, Detroit, MI, USA

[2]Department of Neurology, Henry Ford Hospital, Detroit, MI, USA

[3]Department of Physics, Oakland University, Rochester, MI, USA

Abstract

The beneficial effects of simvastatin on experimental traumatic brain injury (TBI) have been demonstrated in previous studies. In this study, we investigated the effects of simvastatin on axonal injury and neurite outgrowth after experimental TBI and explored the underlying mechanisms. Wistar rats were subjected to controlled cortical impact or sham surgery. Saline or simvastatin was administered for 14 days. A modified neurological severity score (mNSS) test was performed to evaluate functional recovery. Immunohistochemistry studies using synaptophysin, neurofilament H (NF-H) and amyloid-β precursor protein (APP) were performed to examine synaptogenesis and axonal injury. Primary cortical neurons (PCNs) were subjected to oxygen glucose deprivation (OGD) followed by various treatments. Western blot analysis was utilized to assess the activation of phosphatidylinositol-3 kinase (PI-3K)/Akt/mammalian target of rapamycin (mTOR) and glycogen synthase kinase 3β (GSK- 3β)/adenomatous polyposis coli (APC) pathways. Simvastatin decreased the density of APP-positive profiles and increased the density of NF-H -positive profiles. Simvastatin reduced mNSS, which was correlated with the increase of axonal density. Simvastatin treatment stimulated the neurite outgrowth of PCNs after OGD, which was attenuated by LY294002 and enhanced by lithium chloride (LiCl). Simvastatin activated Akt and mTOR, inactivated GSK-3β and dephosphorylated APC in the injured PCNs. Our data suggest that simvastatin reduces axonal injury, enhances neurite outgrowth and promotes neurological functional recovery after experimental TBI. The beneficial effects of simvastatin on neurite outgrowth may be mediated through manipulation of the PI-3K/Akt/mTOR and PI-3K/GSK-3β/APC pathways.

Keywords

axonal injury; glycogen synthase kinase 3β; neurite outgrowth; simvastatin; traumatic brain injury

Address correspondence and reprint requests to: Asim Mahmood, MD Henry Ford Hospital Department of Neurosurgery, E&R Bldg 3072 2799 West Grand Blvd Detroit, MI 48202 Phone: 313-916-3347 Fax: 313-916-7139 nsaam@neuro.hfh.edu.

1. Introduction

Diffuse axonal injury is well documented after head injury and is a major cause of long-term severe disability after traumatic brain injury (TBI) (Adams et al., 1989; Graham et al., 2000). Secondary injury, defined as a cascade of downstream events following initial mechanical injury, is a leading cause of axonal degeneration after TBI (Fitzpatrick et al., 1998). Axons undergo a sequence of changes following a primary insult that culminate in a secondary axotomy over a period of time (Maxwell et al., 1997). Theoretically, this process could be arrested or slowed, making therapies directed against axonal injury applicable during the time course of injury. Amyloid-β precursor protein (APP) is a membrane spanning glycoprotein of nerve cells which is transported by fast axoplasmic flow and accumulates after axonal damage (Koo et al., 1990). APP immunohistochemistry has been shown to be an effective marker for axonal damage (Blumbergs et al., 1995; Bramlett et al., 1997).

Axons in the central nervous system (CNS) of mature animals undergo little spontaneous regeneration (Di Giovanni, 2009). The failure of severed adult CNS axons to regenerate could be attributed to both a reduced intrinsic capacity to grow and a heightened susceptibility to inhibitory factors of the CNS extracellular environment (Teng and Tang, 2006). Recent data support the hypothesis that diminished intrinsic regenerative ability of mature neurons is a major contributor to regeneration failure (Sun and He, 2010). As axonal injury and regeneration play a major role in functional recovery after TBI, several therapeutic strategies to date have been advanced targeting this important pathological process (Buki et al., 1999; Marion and White, 1996; Mills et al., 2011; Singleton et al., 2001).

Given the heterogeneous nature of TBI involving complex primary and secondary events, an ideal TBI therapy should target multiple injury factors. Our previous studies, and those of other researchers, have shown that simvastatin, independent of its cholesterol-lowering activity, mediates pleiotropic effects including modulation of neuroinflammation (Wu et al., 2010) and increase of cerebral blood flow (Cucchiara and Kasner, 2001) in the acute phase, suppression of apoptosis (Wu et al., 2008b) and reduction of excitotoxic death (Zacco et al., 2003) in the subacute phase, and induction of neurogenesis (Wu et al., 2008a) and angiogenesis (Wu et al., 2011) in the chronic phase after TBI. Recent studies also indicate that combination therapies of simvastatin with other agents attenuate axonal damage after CNS injury (Chauhan and Gatto, 2010; Shehadah et al., 2010). In light of these previous studies, simvastatin may be a promising candidate for TBI therapy.

In axon regeneration some distinct intracellular signaling pathways are recruited including the PI-3K/Akt pathway (Goold and Gordon-Weeks, 2004; Read and Gorman, 2009). In this pathway, GSK-3β is one of the key downstream regulators of axon growth. By formation of GSK-3β/APC complex, GSK-3β controls the microtubule-associated protein APC and regulates the microtubule dynamics during axon growth (Votin et al., 2005). As another important downstream target of PI-3K/Akt pathway, mTOR also plays a vital role in the intrinsic axonal regrowth of adult neurons. Activating mTOR induces extensive axon regeneration by promoting protein synthesis in the injured neurons (Park et al., 2008).

In this study we investigate the effect of simvastatin on axonal injury and neurite outgrowth after experimental TBI. To examine possible mechanisms underlying the beneficial effects of simvastatin, we focus on the PI-3K/Akt/mTOR and PI-3K/GSK-3β/APC pathways, which have been implicated as key intrinsic signaling pathways for axon regeneration (Barth et al., 2008; Park et al., 2008).

2. Results

2.1 Neurological outcomes after experimental TBI

Neurological functional deficits caused by injury in the left hemispheric cortex of rats were measured by mNSS (Fig. 1). Injury induced an mNSS score of approximately 12 at 1 day post TBI. Recovery began on day 3 after TBI and persisted for up to 14 days. Simvastatin treatment significantly reduced the mNSS compared to the saline treatment group at day 7 (ANOVA $P = 0.001$; Sim vs Saline: 6.1 ± 0.6 vs 8.4 ± 0.7, $P = 0.028$) and day 14 (ANOVA $P < 0.001$; Sim vs Saline: 5.2 ± 0.4 vs 7.3 ± 0.5, $P = 0.012$) post TBI (Fig. 1).

2.2 Change of axonal damage and synaptic density after simvastatin treatment

APP immunohistochemical staining was performed to measure the traumatic axonal injury (Culmsee et al.) in the injured brain. TBI induced a marked appearance of APP immunoreactivity in cortical perikarya and axons. Simvastatin significantly decreased the density of APP positive axons in the ipsilateral hemisphere compared with saline-treated group (Fig. 2I-L, ANOVA $P < 0.001$, simvastatin vs saline, $P = 0.021$). In addition, axons were identified by fluorescent immunostaining of a pan-axonal NF-H marker, SMI-312, and by Bielschowsky silver staining. Simvastatin treatment significantly increased the density of NF-H-positive axons in the lesion boundary zone (Fig. 2E-H, ANOVA $P < 0.001$, simvastatin vs saline, $P = 0.007$) and density of Bielschowsky silver-positive axons in the striatal bundles (Fig. 2M-P, ANOVA $P < 0.001$, simvastatin vs saline, $P = 0.015$). Synaptophysin was employed to measure the level of synapses after TBI. TBI led to loss of synapses in the lesion boundary zone, which was partially reversed by treatment of simvastatin. Quantitative analysis revealed that simvastatin increased the density of synaptophysin in the ipsilateral hemisphere compared to the saline-treated group (Fig. 2A-D, ANOVA $P = 0.005$, simvastatin vs saline, $P = 0.037$).

To confirm the above effects of simvastatin, brain tissues from lesion boundary zone were harvested and Western blot analysis was employed to measure semi-quantitatively the levels of NF-H, APP and synaptophysin. Simvastatin suppressed the expression of APP while increasing the levels of NF-H and synaptophysin 14 days after injury (Fig. 3). These data confirmed that simvastatin reduced axonal injury and increased axonal and synaptic density post TBI.

2.3 Correlation of axonal density and functional outcome after TBI

To investigate whether simvastatin-induced increase of axonal density is correlated with functional outcome in rats, Pearson's correlation coefficient was performed to analyze the relationship between the mNSS score and axonal density at 14 days after TBI. Our data showed that the score of mNSS was significantly inversely correlated with the axonal density of ipsilateral hemisphere (Fig. 4). The correlation coefficient was -0.98 ($P = 0.008$).

2.4 Impact of PI3K inhibition on simvastatin-induced neurite outgrowth in the injured PCNs

PCNs were subjected to oxygen glucose deprivation (OGD) and treated with vehicle control, simvastatin, simvastatin + cholesterol, simvastatin + LiCl (GSK-3β inhibitor) or simvastatin + LY294002 (PI-3K inhibitor). TUJ-1 immunostaining was performed to identify neurons and neurite outgrowth. Figure 5 shows that simvastatin significantly increased neurite outgrowth compared with vehicle control in the injured PCNs (Fig. 5B,C&G, $P = 0.015$, O + S vs OGD). Neurite outgrowth was not altered with a cholesterol supplement, suggesting that the effect of simvastatin was independent of cholesterol change. Simvastatin-induced neurite outgrowth was abolished by LY294002 (Fig. 5F&G, $P = 0.022$, O + S+ LY vs O + S) and enhanced by LiCl (Fig. 5E&G, $P = 0.006$, O + S + LiCl vs O + S).

2.5 PI-3K/Akt/mTOR and PI-3K/GSK-3 /APC pathways and neurite outgrowth after OGD

PCNs were subjected to OGD and followed by various treatments. Neurons were harvested 24 h later and Western blot analysis was performed to evaluate the protein expression of p-Akt, p-mTOR, p-GSK-3β and APC. ELISA was performed to assess the level of phosphorylated APC. Quantitative analysis of protein expression suggested that simvastatin treatment promoted the phosphorylation of Akt, mTOR and GSK-3β in the injured neurons (Fig. 6A). As the GSK-3β/APC complex plays a crucial role in neurite outgrowth, we also examined the level of APC. Simvastatin increased the level of dephosphorylated APC in the injured neurons. Cholesterol supplement did not alter the effect of simvastatin. Inhibition of GSK-3 β with LiCl significantly enhanced APC level (Fig. 6A & C, $P = 0.034$, O + S + LiCl vs O + S). Inhibition of PI3K/Akt with LY294002 reversed the effects of simvastatin on p-mTOR, p-GSK-3β and APC (Fig. 6A & C). In addition, simvastatin reduced the level of phospho-APC in the injured PCNs. This simvastatin-induced phospho-APC reduction was enhanced by LiCl but reversed by LY294002.

3.0 Discussion

The primary findings in this study are: 1) Treatment of simvastatin attenuated axonal injury and increased axonal density, which was correlated to functional recovery after experimental TBI; and 2) Simvastatin monotherapy enhanced in vitro neurite outgrowth in the injured immature PCNs, which may be mediated by manipulation of the PI-3K/Akt/mTOR and PI-3K /GSK-3β/APC pathways.

We used a modified controlled cortical impact (CCI) model for this study since it reproduces many of the features observed in TBI including axonal injury and simulates the occurrence of closed-head injury in clinical settings (Dixon et al., 1991). Traumatic axonal injury (Culmsee et al.) is a major contributor to TBI evoked morbidity (Kelley et al., 2006; Lipton et al., 2008). Experimental TBI induces a progressive temporal course of axonal injury which begins within an hour of injury with a subsequent and rapid increase in the extent and distribution over the following hours. Maximal axon swelling is present at 80 h post injury (Gorrie et al., 2002). The progression of axonal injury involves a complex sequence of changes including calcium influx, disruption of neurofilament cytoskeleton, delayed rupture of axon membrane, and a final irreversible disconnection of axon (Povlishock and Christman, 1995). This progressive temporal course provides an early window of opportunity for axon-targeted treatment (Povlishock, 2000). In the current study, we used APP immunohistochemical staining to identify the damaged axons. APP immunohistochemistry has been shown to be a more effective and sensitive method for visualizing axonal injury than other immunohistochemical methods (Blumbergs et al., 1995; Sherriff et al., 1994). In our results, the neuropathological appearance of injured axons including axonal enlargement, beading, and spheroids was most commonly seen in the deep layers of the neocortex, parasagittal white matter and corpus callosum, while there was less staining in superficial cortical neurons and central gray matter. When combined with other agents, simvastatin has been shown to attenuate the axonal damage after stroke (Chauhan and Gatto, 2010; Shehadah et al., 2010). In addition, simvastatin induces neurite outgrowth in PC12 cells (Sato-Suzuki and Murota, 1996). In light of these previous studies we investigated the effect of simvastatin monotherapy on the axonal injury and neurite outgrowth after TBI. Since simvastatin is lipophilic, it has a higher blood-brain-barrier permeability than other hydrophilic statins (Saheki et al., 1994). Simvastatin treatment significantly reduced the density of APP-positive profiles in the traumatized hemisphere (Fig. 2 I-L), suggesting that simvastatin attenuated TAI after TBI. Western blot analysis using tissues from ipsilateral hemisphere confirmed the downregulated APP expression after simvastatin treatment (Fig. 3). Density of axons in the traumatized hemisphere 14 days after TBI was significantly increased with simvastatin treatment (Figure 2 E-H & M-P), which

was correlated to the scores of mNSS (Fig. 4) compared to the sham- and saline-treated groups. However, this correlation between various groups needs to be further validated by larger sample studies as an inverse correlation seems to exist within each group.

Increase of axonal density after simvastatin treatment may be attributed to the attenuated axonal injury and/or the enhanced axon regeneration after TBI. To further elucidate the effect of simvastatin on axonal regeneration, cultured PCNs were subjected to hypoxic injury with OGD since the post-traumatic ischemia plays a major role in the secondary injury after TBI. To treat the cells 1 uM simvastatin was used, and this dosage was chosen based on previous studies showing that simvastatin at a lower dose exhibits neuroprotective effects (Kureishi et al., 2000; Wu et al., 2011). Simvastatin significantly increased the length of neurite outgrowth in the injured neurons compared to the vehicle control (Fig. 5A). Simvastatin-induced neurite outgrowth was inhibited by LY29402; enhanced by LiCl, and not altered by cholesterol supplement (Fig. 5A&B). These data suggest that simvastatin-induced neurite outgrowth is related to the PI-3k/GSK-3β signaling pathway and is independent of cholesterol change. However, as PCNs are harvested from E17 rats, they are immature neurons. It is unclear whether the developmental programs that regulate axonal growth have stopped in the PCNs. Therefore simvastatin-induced neurite outgrowth could also be attributed to the developmental program changes in addition to the promoted axonal regeneration. One of the limitations of the current study is that we utilized OGD as the *in vitro* injury model, which, however, does not completely represent the pathophysiological changes after experimental TBI. In addition to lack of hemorrhage and the breakdown of the blood brain barrier, glial cell activation and subsequent inflammations in the *in vitro* OGD model hinder the interpretation and translation of *in vitro* data into the *in vivo* TBI model.

Low CNS axonal regeneration ability could be attributed to both a reduced intrinsic capacity to grow and an elevated susceptibility to inhibitory factors such as myelin-associated inhibitory molecules (Sun and He, 2010). Recent studies revealed that simply removing inhibitory factors is insufficient for successful axon regeneration (Lee et al., 2009; Yiu and He, 2006) while collective experimental evidence suggests that activating intrinsic pathways may be an alternative and complementary approach (Di Giovanni, 2009). Therefore, manipulation of downstream molecules that are more directly involved in axonal regeneration mechanisms is a potentially attractive and effective approach. To date, the intracellular mechanisms that maintain and regulate axon growth are not well understood. Two transcription factors, the cyclic AMP response element binding protein (CREB) and signal transducer and activator of transcription 3 (STAT3), have been implicated in the neurite outgrowth (Lonze and Ginty, 2002; Qiu et al., 2005). In addition, previous experiments strongly implicate GSK-3β in the regulation of axonal growth through its substrate microtubule-associated protein APC (Hall et al., 2000; Lucas et al., 1998). GSK-3β is constitutively active in resting cells and must be inactivated by extracellular signals to allow the activation of its substrates (Cohen and Frame, 2001). GSK-3β phosphorylates APC and forms a complex with it, abolishing the ability of APC to bind to microtubule. Inactivation of GSK-3β allows the dephosphorylated APC protein to bind to the microtubule plus ends and therefore promotes microtubule assembly (Votin et al., 2005; Zhou et al., 2004). Another major intrinsic protein for axon regeneration is mTOR, which is highly active in neurons during the course of development. mTOR is less active in adult neurons and is further suppressed after axotomy. The deletion of phosphatase and tensin homolog (PTEN), a negative regulator of the mTOR pathway, promotes robust axonal regeneration after optic nerve injury (Park et al., 2008). As both GSK-3β and mTOR are the downstream targets of PI-3K/Akt pathway, mTOR controls cap-dependent protein translation (Park et al., 2008) and GSK-3β regulates cytoskeleton assembly (Ma et al., 2008) in neurons. Our data show that simvastatin activated Akt and phosphorylates (ie, inactivates) GSK-3β in the injured neurons. Inactivation of GSK-3β, in turn, dephosphorylated and released APC from

the GSK-3β/APC complex (Fig. 6 &7), facilitated APC binding to microtubules and eventually led to increased microtubule stability (Zhou et al., 2004). The activity of GSK-3β is regulated by various phosphorylation sites. Serine phosphorylation of GSK3-beta is inhibitory and allows unphosphorylated APC to promote microtubule assembly. Tyrosine phosphorylation of GSK3-beta further activates the enzyme and promotes APC inhibition. Therefore anti-p-GSK-3β (Ser9) was selected in the current study. Meanwhile, activation of mTOR after simvastatin treatment (Fig. 6) contributed to the neurite outgrowth via upregulation of protein synthesis in the injured neurons. Inhibition of PI-3K with LY294002 and inhibition of GSK-3β with LiCl confirmed that GSK-3β/APC modulation mediated the beneficial effect of simvastatin on neurite outgrowth, and that mTOR is independent of GSK-3β. Therefore, we propose that simvastatin-induced neurite outgrowth in the injured neurons may be attributed to the activation of PI-3K/Akt/mTOR and PI-3K/ GSK-3β/APC pathways (Fig. 7). Although lithium chloride is widely used as a GSK3-beta inhibitor, lithium salts are known to interfere with several other processes of cell homeostasis including amino acid transport, nucleoside transport and the activity of the Na-K ATPase pump (Jope, 1999). These factors may affect the results in the present study.

Compared to the previous reports of statin combination treatment on axonal injury after TBI (Chauhan and Gatto, 2010) or stroke (Shehadah et al., 2010), the current study proves that simvastatin mono-therapy reduces axonal injury. In addition, we investigated the molecular mechanisms underlying the simvastatin-induced neurite outgrowth.

In conclusion, the current study demonstrates that simvastatin monotherapy reduces axonal injury significantly and improves functional outcome after experimental TBI. Simvastatin also promotes neurite outgrowth in the hypoxic embryonic PCNs. The beneficial effect of simvastatin on neurite outgrowth may be mediated by manipulation of the PI-3K/Akt/mTOR and PI-3K /GSK-3β/APC pathways.

4. Experimental Procedure

All experiments were approved by the Institutional Animal Care and Use Committee of Henry Ford Health System (IACUC #0660).

4.1 Animal model and experimental groups

Male Wistar rats (n = 36) were anesthetized with 4% chloral hydrate (350 mg/kg, i.p.). A controlled cortical impact (CCI) device was used to induce injury (Dixon et al., 1991). The rats were placed in a stereotactic frame. Two 10-mm diameter craniotomies were performed adjacent to the central suture, midway between lambda and bregma. The second craniotomy allowed for the lateral movement of brain tissue (Mahmood et al., 2008). Injury was induced by striking the left cortex with a 6-mm-diameter tip pneumatic piston at a rate of 4 m/s and 2.5 mm of compression. Velocity was measured using a linear velocity displacement transducer. Sham-injured animals were similarly anesthetized and craniectomy performed without cortical injury.

Rats were divided randomly into 3 groups. There were 12 rats in each group (n = 12). Rats in Group 1 were subjected to sham surgery. Rats in Group 2 were subjected to TBI and treated with saline orally 1 day later and consecutively for 14 days. Rats in Group 3 were subjected to TBI, and simvastatin was administered orally 1 day later at a dose of 1 mg/kg/day for 14 consecutive days. This dose was selected based on our previously reported study (Wu et al., 2008a). The rats were sacrificed at 14 days after TBI. From each group, 8 rats were used for immunohistochemistry study and the other 4 rats for Western blot analysis.

4.2 Neurological functional evaluation

Neurological functional measurement was performed using a modified Neurological Severity Score (mNSS). A detailed description of this functional test has been described previously (Chen et al., 2001). The test was carried out on all rats pre-injury and at indicated timepoints after TBI. The mNSS is a composite of the motor (muscle status, abnormal movement), sensory (visual, tactile and proprioceptive) and reflex tests. Motor tests of the mNSS include seven items with a maximum of 6 points. Sensory tests include two items with a maximum score of 2. Beam Balance Tests have seven items with a maximum score of 6. The last part of the mNSS includes the pinna, corneal and startle reflexes and abnormal movements. Insult in the left hemisphere cortex of rats causes sensory and motor functional deficiency with elevated scores early after TBI. The tests were performed by observer blinded to individual treatment.

4.3 Tissue preparation

For immunostaining, rats were anesthetized with 4% chloral hydrate i.p. and perfused transcardially with saline followed by 4% paraformaldehyde. Brains were harvested, post-fixed in 4% paraformaldehyde at 4°C for 2 days, and then cut into seven 2-mm-thick standard coronal blocks on a rodent brain matrix. A series of sections were cut with a microtome through each of the seven standard sections. For biochemical analysis, the ipsilateral brain tissues from lesion boundary zone were dissected, frozen in liquid nitrogen and stored at -80°C.

4.4 Immunohistochemistry

After rehydration, tissue sections were treated with 3% H_2O_2 to block endogenous peroxidase activity and then boiled in 1% citric acid buffer (pH 6) in a microwave oven for 10 min. Sections were incubated in 1% BSA for 1 h to block the nonspecific signals. Using the same buffer solution, the sections were incubated overnight at 4°C with primary antibody (ie, anti–synaptophysin 1:1000, Millipore, Billerica, MA; anti-amyloid β [A4] precursor protein [APP] 1:500, Cell Signaling, Beverly, MA; and anti-pan axonal Neurofilament H [SMI-312] 1:1000, Covance, Princeton, NJ). For negative controls, primary antibody was omitted. For NF-H staining, sections were incubated with corresponding fluorochrome-conjugated secondary antibody (fluorescein isothiocyanate; FITC 1:2000, Jackson ImmunoResearch, West Grove, PA) for 2 h at room temperature. For synaptophysin and APP staining, sections were incubated with biotin-conjugated secondary antibody (1:200 dilution, Dakopatts, Carpenteria, CA), followed by incubation with an avidin-biotin-peroxidase system (ABC kit, Vector Laboratories, Inc., Burlingame, CA). DAB was then used as a sensitive chromogen for light microscopy. Tissue sections were mounted with cover slides and Vectashield mounting medium (Vector Laboratories). To detect the axonal fiber tracts, a Bielshowsky's silver and Luxol fast blue staining was performed. Bielshowsky's silver staining was used to show the axons (von Bohlen und Halbach and Albrecht, 1998) and Luxol fast blue staining for myelin (Salthouse, 1964). For Bielshowsky's silver staining, sections were incubated in 20% silver nitrate in the dark, followed by ammonium hydroxide until the tissues turned brown with a gold background, and then sodium thiosulfate was added. Finally, sections were stained in Luxol fast blue, washed in 95% alcohol and placed in lithium carbonate. Myelin is blue and axons appear as black.

For quantitative measurement of the density of immunoreactive area, microphotographs from the lesion boundary zone were digitized under a x20 objective using a 3-CCD color camera (Nikon, Tokyo, Japan) interfaced with an Micro Computer Imaging Device (MCID) image analysis system (Imaging Research, St. Catharine's, ON, Canada) (Calza et al., 2001; Chen et al., 2003). We drew the lesion boundary zone areas on coronal sections at a low

objective. A higher power was then selected, and the MCID system used random systematic sampling to sample 30% of the defined region. When the system moved to the first location within the region of interest, a counting frame was placed over the selected area. We then counted the number of immunostained cells within the counting frame. The data collected from five sections and eight fields within each section were averaged to obtain a single value for one animal and were presented as the percentage of positive area for synaptophysin, NF-H, APP, and Bielschowsky silver immunoreactive profiles. Data were analyzed by a researcher who was blinded to the animal grouping.

4.5 In Vitro OGD/reoxygenation model

Neurons were seeded in each well of a 6-well plate containing normal neurobasal medium (Invitrogen, Carlsbad, CA, USA) until they attached to the plate. Normal neurobasal medium was then replaced with DMEM without glucose, and the cells were incubated in an anaerobic chamber (model 1025; Forma Scientific, Marietta, OH) for 1 h. The oxygen level within the anaerobic chamber was routinely measured with a BD Disposable Anaerobic Indicator (Becton, Dickinson and Company, Sparks, MD), which confirmed that the oxygen level remained below 0.2%. After OGD, glucose-free DMEM was replaced with normal neurobasal medium and the cells were incubated under normal culture conditions. Simvastatin or other agents were added at the start of OGD and maintained during the reoxygenation process. After 24 h, cells were detached and collected for further study.

4.6 Primary cortical neuron culture and neurite outgrowth measurements

To test the effect of simvastatin on neurite outgrowth, PCNs were harvested from embryonic day 17 fetal rats and cultured in the neurobasal medium (Invitrogen) supplemented with B27 for 5 days. Culture dishes were pre-coated with poly D-lysine solution and left in the incubator overnight at 37°C in an atmosphere of 95% air and 5% carbon dioxide . For image analysis 6×10^3 cells were plated per well to the chambered slides, and for Western blot analysis 6×10^6 cells were plated per 10-cm culture dish. Immunofluorescent staining for TUJ1 (β-tubulin III) was performed to identify the neurons, and a 91% purity of neurons was calculated. PCNs were then subjected to 1 h of OGD, followed by 23 h of re-oxygenation. Hypoxic PCNs were subsequently treated with vehicle control, simvastatin (1 μM), simvastatin with cholesterol, simvastatin with GSK-3 activation inhibitor LiCl (3 mM), or simvastatin with LY294002 (10 μM). Lithium chloride (LiCl) potently inhibits GSK-3 beta activity (Ki = 2 mM) (Klein and Melton, 1996). The potency of Li(+) inhibition is dependent on Mg(2+) concentration (Ryves and Harwood, 2001). LY294002 is a potent reversible inhibitor of PI3K. It specifically abolished PI3 kinase activity (IC50=0.43 μg/ml; 1.40 μM) but did not inhibit other lipid and protein kinases. Y294002 has been shown to block PI3 kinase-dependent Akt phosphorylation and kinase activity (Vlahos et al., 1994). Profiles of neurons were identified with fluorescent immunostaining using TUJ1 for neurite outgrowth measurement. TUJ1 labeled neurons were observed under a fluorescent microscope (Nikon) and photomicrographs were captured at x200 magnification using a 3 CCD digital camera (Nikon). A total of 20 neurons were captured in each well. The total neurite outgrowth length was measured in 20 neurons using the MCID analysis system. The total length of 20 neurons was averaged and the mean value was presented in each well. Four wells were used in each group (n = 4).

4.7 Western blot analysis

Rats were sacrificed at day 14 after TBI (n = 4). Brain tissue from lesion boundary zones was collected, washed once in 1x phosphate-buffered saline (PBS) and lysed in lysis buffer (20 mM Tris pH 7.6, 100 mM NaCl, 1% Nonidet P-40, 0.1% SDS, 1% deoxycholic acid, 10% glycerol, 1 mM EDTA, 1 mM $NaVO_3$, 50 mM NaF, cocktail I of protease inhibitors from Calbiochem). After sonication, soluble protein was obtained by centrifugation at

13,000 × g for 15 min at 4° C. In the *in vitro* study, cells were collected from the wells (n = 4) after various treatments and washed once with 1x PBS and lysed in lysis buffer on ice for 30 min. Tissue or cell lysates were prepared and their protein concentrations were determined with bicinchoninic acid (BCA) protein assay (Pierce, Rockford, IL). Equal amounts of lysate were subjected to SDS-polyacrylamide electrophoresis on Novex tris-glycine pre-cast gels (Invitrogen) and separated proteins were then electrotransferred to polyvinylidene fluoride (PVDF) membranes (Millipore, Bedford, MA). After exposure to various antibodies, specific proteins were visualized using SuperSignal West Pico chemiluminescence substrate system (Pierce Rockford, IL). The band intensity was analyzed using Scion Image software (Scion, Frederick, MD). Antibodies used for Western blot included anti-synaptophysin (Millipore), anti-APP (Cell Signaling), anti-pan axonal Neurofilament H (SMI-312) (Covance), anti-p-Akt (Ser473) (Cell Signaling), anti-p-GSK-3β (Ser9) (Cell Signaling), anti-p-mTOR (Ser2448) (Cell Signaling), anti-APC (Abcam, Cambridge, MA), and anti-actin (Santa Cruz Biotechnology, Santa Cruz, CA).

4.8 Enzyme-Linked ImmunoSorbent Assay (ELISA)

Using anti-p-APC (ser2054) antibody (Abcam), levels of phosphorylated APC were measured using equal amounts of lysate from variously treated PCN samples. Each well of a PVC microtiter plate was coated with 50 μl of lysate at final concentration of 20 μg/ml in carbonate coating buffer. The plate was covered and incubated at 4°C overnight. The coating solution was removed and wells were washed with PBS three times. 200 μl of blocking buffer was applied into each well for 2 h at room temperature, followed by PBS washing. 100 μl of anti-p-APC (ser2054) antibody (1:4000 dilution) was added in each well and the plate was incubated at 4°C overnight. 100 μl of substrate solution was dispensed to each well for 30 min and followed by stop solution. The optical density of each well was read with a plate reader.

4.9 Statistical analyses

All data are presented as mean with standard deviations (SD). Data were analyzed by repeated measurements analysis of variance (Kavanova and Gloser) for mNSS. For immunohistochemical staining and immunoblotting, a one-way ANOVA test followed by a post hoc Student-Newman-Keuls (SNK) test was used to compare the difference between groups. Pearson Correlation was used to analyze the correlation between functional outcome and axonal density. Statistical significance was present when *P* values were less than 0.05.

Acknowledgments

Disclosure of funding

This work was supported by National Institutes of Health (NIH) grants R01NS052280-01A1 (A.M.), and R01AG037506 (M.C.)

References

Adams JH, Doyle D, Ford I, Gennarelli TA, Graham DI, McLellan DR. Diffuse axonal injury in head injury: definition, diagnosis and grading. Histopathology. 1989; 15:49–59. [PubMed: 2767623]

Barth AI, Caro-Gonzalez HY, Nelson WJ. Role of adenomatous polyposis coli (APC) and microtubules in directional cell migration and neuronal polarization. Semin Cell Dev Biol. 2008; 19:245–251. [PubMed: 18387324]

Blumbergs PC, Scott G, Manavis J, Wainwright H, Simpson DA, McLean AJ. Topography of axonal injury as defined by amyloid precursor protein and the sector scoring method in mild and severe closed head injury. J Neurotrauma. 1995; 12:565–572. [PubMed: 8683607]

Bramlett HM, Kraydieh S, Green EJ, Dietrich WD. Temporal and regional patterns of axonal damage following traumatic brain injury: a beta-amyloid precursor protein immunocytochemical study in rats. J Neuropathol Exp Neurol. 1997; 56:1132–1141. [PubMed: 9329457]

Buki A, Okonkwo DO, Povlishock JT. Postinjury cyclosporin A administration limits axonal damage and disconnection in traumatic brain injury. J Neurotrauma. 1999; 16:511–521. [PubMed: 10391367]

Calza L, Giardino L, Giuliani A, Aloe L, Levi-Montalcini R. Nerve growth factor control of neuronal expression of angiogenetic and vasoactive factors. Proc Natl Acad Sci U S A. 2001; 98:4160–4165. [PubMed: 11259645]

Chauhan NB, Gatto R. Synergistic benefits of erythropoietin and simvastatin after traumatic brain injury. Brain Res. 2010; 1360:177–192. [PubMed: 20833152]

Chen J, Sanberg PR, Li Y, Wang L, Lu M, Willing AE, Sanchez-Ramos J, Chopp M. Intravenous administration of human umbilical cord blood reduces behavioral deficits after stroke in rats. Stroke. 2001; 32:2682–2688. [PubMed: 11692034]

Chen J, Zhang ZG, Li Y, Wang Y, Wang L, Jiang H, Zhang C, Lu M, Katakowski M, Feldkamp CS, Chopp M. Statins induce angiogenesis, neurogenesis, and synaptogenesis after stroke. Ann Neurol. 2003; 53:743–751. [PubMed: 12783420]

Cohen P, Frame S. The renaissance of GSK3. Nat Rev Mol Cell Biol. 2001; 2:769–776. [PubMed: 11584304]

Cucchiara B, Kasner SE. Use of statins in CNS disorders. J Neurol Sci. 2001; 187:81–89. [PubMed: 11440749]

Culmsee C, Siewe J, Junker V, Retiounskaia M, Schwarz S, Camandola S, El-Metainy S, Behnke H, Mattson MP, Krieglstein J. Reciprocal inhibition of p53 and nuclear factor-kappaB transcriptional activities determines cell survival or death in neurons. J Neurosci. 2003; 23:8586–8595. [PubMed: 13679428]

Di Giovanni S. Molecular targets for axon regeneration: focus on the intrinsic pathways. Expert Opin Ther Targets. 2009; 13:1387–1398. [PubMed: 19922299]

Dixon CE, Clifton GL, Lighthall JW, Yaghmai AA, Hayes RL. A controlled cortical impact model of traumatic brain injury in the rat. J Neurosci Methods. 1991; 39:253–262. [PubMed: 1787745]

Fitzpatrick MO, Maxwell WL, Graham DI. The role of the axolemma in the initiation of traumatically induced axonal injury. J Neurol Neurosurg Psychiatry. 1998; 64:285–287. [PubMed: 9527135]

Goold RG, Gordon-Weeks PR. Glycogen synthase kinase 3beta and the regulation of axon growth. Biochem Soc Trans. 2004; 32:809–811. [PubMed: 15494021]

Gorrie C, Oakes S, Duflou J, Blumbergs P, Waite PM. Axonal injury in children after motor vehicle crashes: extent, distribution, and size of axonal swellings using beta-APP immunohistochemistry. J Neurotrauma. 2002; 19:1171–1182. [PubMed: 12427326]

Graham DI, McIntosh TK, Maxwell WL, Nicoll JA. Recent advances in neurotrauma. J Neuropathol Exp Neurol. 2000; 59:641–651. [PubMed: 10952055]

Hall AC, Lucas FR, Salinas PC. Axonal remodeling and synaptic differentiation in the cerebellum is regulated by WNT-7a signaling. Cell. 2000; 100:525–535. [PubMed: 10721990]

Jope RS. Anti-bipolar therapy: mechanism of action of lithium. Mol Psychiatry. 1999; 4:117–128. [PubMed: 10208444]

Kavanova M, Gloser V. The use of internal nitrogen stores in the rhizomatous grass Calamagrostis epigejos during regrowth after defoliation. Ann Bot. 2005; 95:457–463. [PubMed: 15598700]

Kelley BJ, Farkas O, Lifshitz J, Povlishock JT. Traumatic axonal injury in the perisomatic domain triggers ultrarapid secondary axotomy and Wallerian degeneration. Exp Neurol. 2006; 198:350–360. [PubMed: 16448652]

Klein PS, Melton DA. A molecular mechanism for the effect of lithium on development. Proc Natl Acad Sci U S A. 1996; 93:8455–8459. [PubMed: 8710892]

Koo EH, Sisodia SS, Archer DR, Martin LJ, Weidemann A, Beyreuther K, Fischer P, Masters CL, Price DL. Precursor of amyloid protein in Alzheimer disease undergoes fast anterograde axonal transport. Proc Natl Acad Sci U S A. 1990; 87:1561–1565. [PubMed: 1689489]

Kureishi Y, Luo Z, Shiojima I, Bialik A, Fulton D, Lefer DJ, Sessa WC, Walsh K. The HMG-CoA reductase inhibitor simvastatin activates the protein kinase Akt and promotes angiogenesis in normocholesterolemic animals. Nat Med. 2000; 6:1004–1010. [PubMed: 10973320]

Lee JK, Chan AF, Luu SM, Zhu Y, Ho C, Tessier-Lavigne M, Zheng B. Reassessment of corticospinal tract regeneration in Nogo-deficient mice. J Neurosci. 2009; 29:8649–8654. [PubMed: 19587271]

Lipton ML, Gellella E, Lo C, Gold T, Ardekani BA, Shifteh K, Bello JA, Branch CA. Multifocal white matter ultrastructural abnormalities in mild traumatic brain injury with cognitive disability: a voxel-wise analysis of diffusion tensor imaging. J Neurotrauma. 2008; 25:1335–1342. [PubMed: 19061376]

Lonze BE, Ginty DD. Function and regulation of CREB family transcription factors in the nervous system. Neuron. 2002; 35:605–623. [PubMed: 12194863]

Lucas FR, Goold RG, Gordon-Weeks PR, Salinas PC. Inhibition of GSK-3beta leading to the loss of phosphorylated MAP-1B is an early event in axonal remodelling induced by WNT-7a or lithium. J Cell Sci. 1998; 111(Pt 10):1351–1361. [PubMed: 9570753]

Ma XM, Yoon SO, Richardson CJ, Julich K, Blenis J. SKAR links pre-mRNA splicing to mTOR/S6K1-mediated enhanced translation efficiency of spliced mRNAs. Cell. 2008; 133:303–313. [PubMed: 18423201]

Mahmood A, Goussev A, Lu D, Qu C, Xiong Y, Kazmi H, Chopp M. Long-lasting benefits after treatment of traumatic brain injury (TBI) in rats with combination therapy of marrow stromal cells (MSCs) and simvastatin. J Neurotrauma. 2008; 25:1441–1447. [PubMed: 19072586]

Marion DW, White MJ. Treatment of experimental brain injury with moderate hypothermia and 21-aminosteroids. J Neurotrauma. 1996; 13:139–147. [PubMed: 8965323]

Maxwell WL, Povlishock JT, Graham DL. A mechanistic analysis of nondisruptive axonal injury: a review. J Neurotrauma. 1997; 14:419–440. [PubMed: 9257661]

Mills JD, Bailes JE, Sedney CL, Hutchins H, Sears B. Omega-3 fatty acid supplementation and reduction of traumatic axonal injury in a rodent head injury model. J Neurosurg. 2011; 114:77–84. [PubMed: 20635852]

Park KK, Liu K, Hu Y, Smith PD, Wang C, Cai B, Xu B, Connolly L, Kramvis I, Sahin M, He Z. Promoting axon regeneration in the adult CNS by modulation of the PTEN/mTOR pathway. Science. 2008; 322:963–966. [PubMed: 18988856]

Povlishock JT. Pathophysiology of neural injury: therapeutic opportunities and challenges. Clin Neurosurg. 2000; 46:113–126. [PubMed: 10944671]

Povlishock JT, Christman CW. The pathobiology of traumatically induced axonal injury in animals and humans: a review of current thoughts. J Neurotrauma. 1995; 12:555–564. [PubMed: 8683606]

Qiu J, Cafferty WB, McMahon SB, Thompson SW. Conditioning injury-induced spinal axon regeneration requires signal transducer and activator of transcription 3 activation. J Neurosci. 2005; 25:1645–1653. [PubMed: 15716400]

Read DE, Gorman AM. Involvement of Akt in neurite outgrowth. Cell Mol Life Sci. 2009; 66:2975–2984. [PubMed: 19504044]

Ryves WJ, Harwood AJ. Lithium inhibits glycogen synthase kinase-3 by competition for magnesium. Biochem Biophys Res Commun. 2001; 280:720–725. [PubMed: 11162580]

Saheki A, Terasaki T, Tamai I, Tsuji A. In vivo and in vitro blood-brain barrier transport of 3-hydroxy-3-methylglutaryl coenzyme A (HMG-CoA) reductase inhibitors. Pharm Res. 1994; 11:305–311. [PubMed: 8165193]

Salthouse TN. Luxol Fast Blue G as a Myelin Stain. Stain Technol. 1964; 39:123. [PubMed: 14127797]

Sato-Suzuki I, Murota S. Simvastatin inhibits the division and induces neurite-like outgrowth in PC12 cells. Neurosci Lett. 1996; 220:21–24. [PubMed: 8977139]

Shehadah A, Chen J, Cui X, Roberts C, Lu M, Chopp M. Combination treatment of experimental stroke with Niaspan and Simvastatin, reduces axonal damage and improves functional outcome. J Neurol Sci. 2010; 294:107–111. [PubMed: 20451219]

Sherriff FE, Bridges LR, Gentleman SM, Sivaloganathan S, Wilson S. Markers of axonal injury in post mortem human brain. Acta Neuropathol. 1994; 88:433–439. [PubMed: 7847072]

Singleton RH, Stone JR, Okonkwo DO, Pellicane AJ, Povlishock JT. The immunophilin ligand FK506 attenuates axonal injury in an impact-acceleration model of traumatic brain injury. J Neurotrauma. 2001; 18:607–614. [PubMed: 11437083]

Sun F, He Z. Neuronal intrinsic barriers for axon regeneration in the adult CNS. Curr Opin Neurobiol. 2010; 20:510–518. [PubMed: 20418094]

Teng FY, Tang BL. Axonal regeneration in adult CNS neurons--signaling molecules and pathways. J Neurochem. 2006; 96:1501–1508. [PubMed: 16476081]

Vlahos CJ, Matter WF, Hui KY, Brown RF. A specific inhibitor of phosphatidylinositol 3-kinase, 2-(4-morpholinyl)-8-phenyl-4H-1-benzopyran-4-one (LY294002). J Biol Chem. 1994; 269:5241–5248. [PubMed: 8106507]

von Bohlen und Halbach O, Albrecht D. Tracing of axonal connectivities in a combined slice preparation of rat brains--a study by rhodamine-dextran-amine-application in the lateral nucleus of the amygdala. J Neurosci Methods. 1998; 81:169–175. [PubMed: 9696322]

Votin V, Nelson WJ, Barth AI. Neurite outgrowth involves adenomatous polyposis coli protein and beta-catenin. J Cell Sci. 2005; 118:5699–5708. [PubMed: 16303851]

Wu H, Jiang H, Lu D, Qu C, Xiong Y, Zhou D, Chopp M, Mahmood A. Induction of angiogenesis and modulation of vascular endothelial growth factor receptor-2 by simvastatin after traumatic brain injury. Neurosurgery. 2011; 68:1363–1371. discussion 1371. [PubMed: 21307798]

Wu H, Lu D, Jiang H, Xiong Y, Qu C, Li B, Mahmood A, Zhou D, Chopp M. Simvastatin-mediated upregulation of VEGF and BDNF, activation of the PI3K/Akt pathway, and increase of neurogenesis are associated with therapeutic improvement after traumatic brain injury. J Neurotrauma. 2008a; 25:130–139. [PubMed: 18260796]

Wu H, Lu D, Jiang H, Xiong Y, Qu C, Li B, Mahmood A, Zhou D, Chopp M. Increase in phosphorylation of Akt and its downstream signaling targets and suppression of apoptosis by simvastatin after traumatic brain injury. J Neurosurg. 2008b; 109:691–698. [PubMed: 18826357]

Wu H, Mahmood A, Lu D, Jiang H, Xiong Y, Zhou D, Chopp M. Attenuation of astrogliosis and modulation of endothelial growth factor receptor in lipid rafts by simvastatin after traumatic brain injury. J Neurosurg. 2010; 113:591–597. [PubMed: 19895202]

Yiu G, He Z. Glial inhibition of CNS axon regeneration. Nat Rev Neurosci. 2006; 7:617–627. [PubMed: 16858390]

Zacco A, Togo J, Spence K, Ellis A, Lloyd D, Furlong S, Piser T. 3-hydroxy-3-methylglutaryl coenzyme A reductase inhibitors protect cortical neurons from excitotoxicity. J Neurosci. 2003; 23:11104–11111. [PubMed: 14657168]

Zhou FQ, Zhou J, Dedhar S, Wu YH, Snider WD. NGF-induced axon growth is mediated by localized inactivation of GSK-3beta and functions of the microtubule plus end binding protein APC. Neuron. 2004; 42:897–912. [PubMed: 15207235]

Highlights

- Simvastatin improves functional outcome after traumatic brain injury (TBI)
- Simvastatin reduces axonal injury and increases axonal density after TBI
- Increased axonal density is correlated with functional recovery after TBI
- Simvastatin significantly stimulates the neurite outgrowth in the primary cortical neurons.

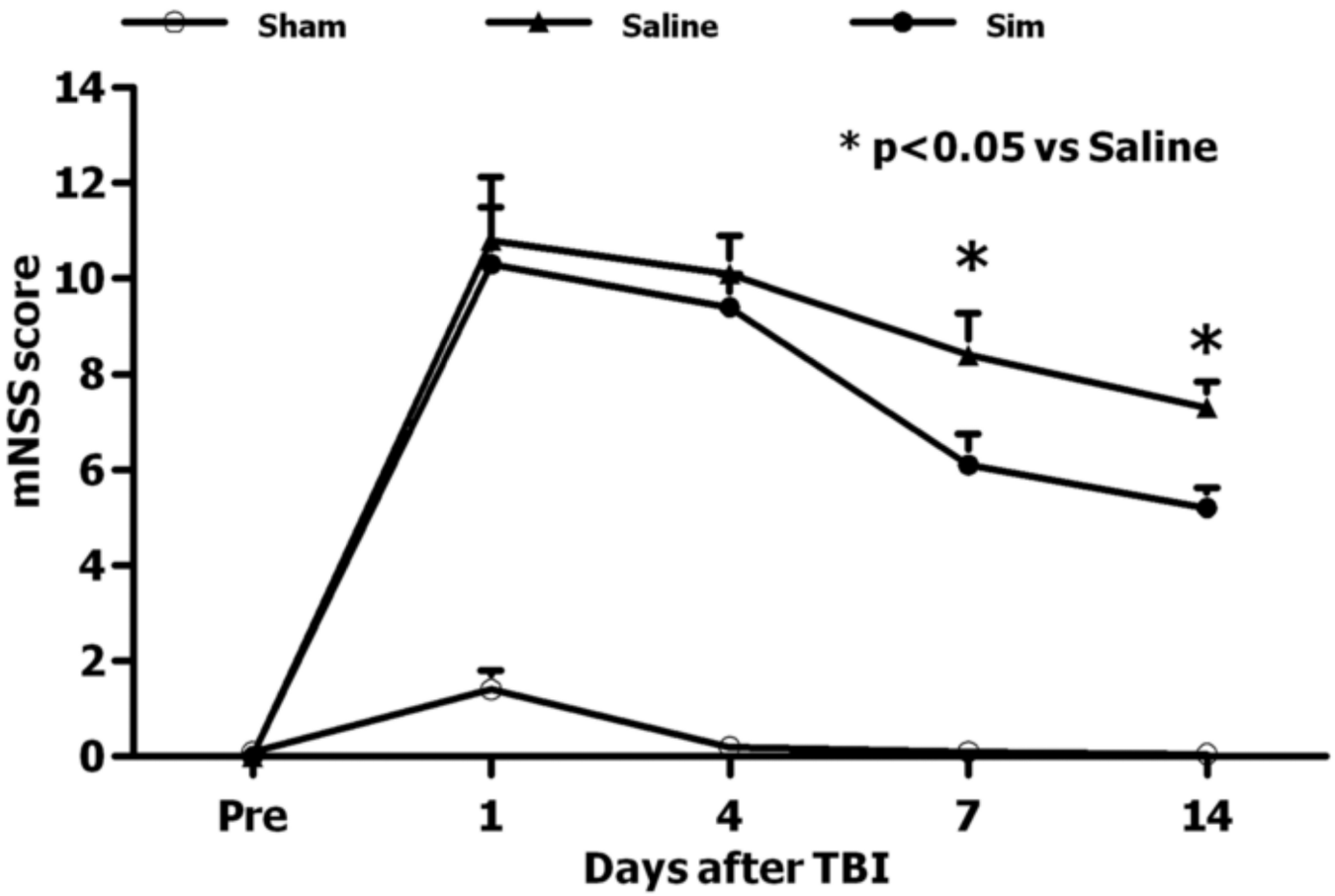

Fig. 1.

Graph showing the effect of simvastatin on functional recovery after TBI. TBI significantly impairs sensory motor function at days 1-14 compared with sham controls. Treatment with simvastatin improves sensorimotor function measured by mNSS at days 7-14 compared with the saline group. Pre = pre-injury level. Data represent the mean ± SD. n = 8/group.

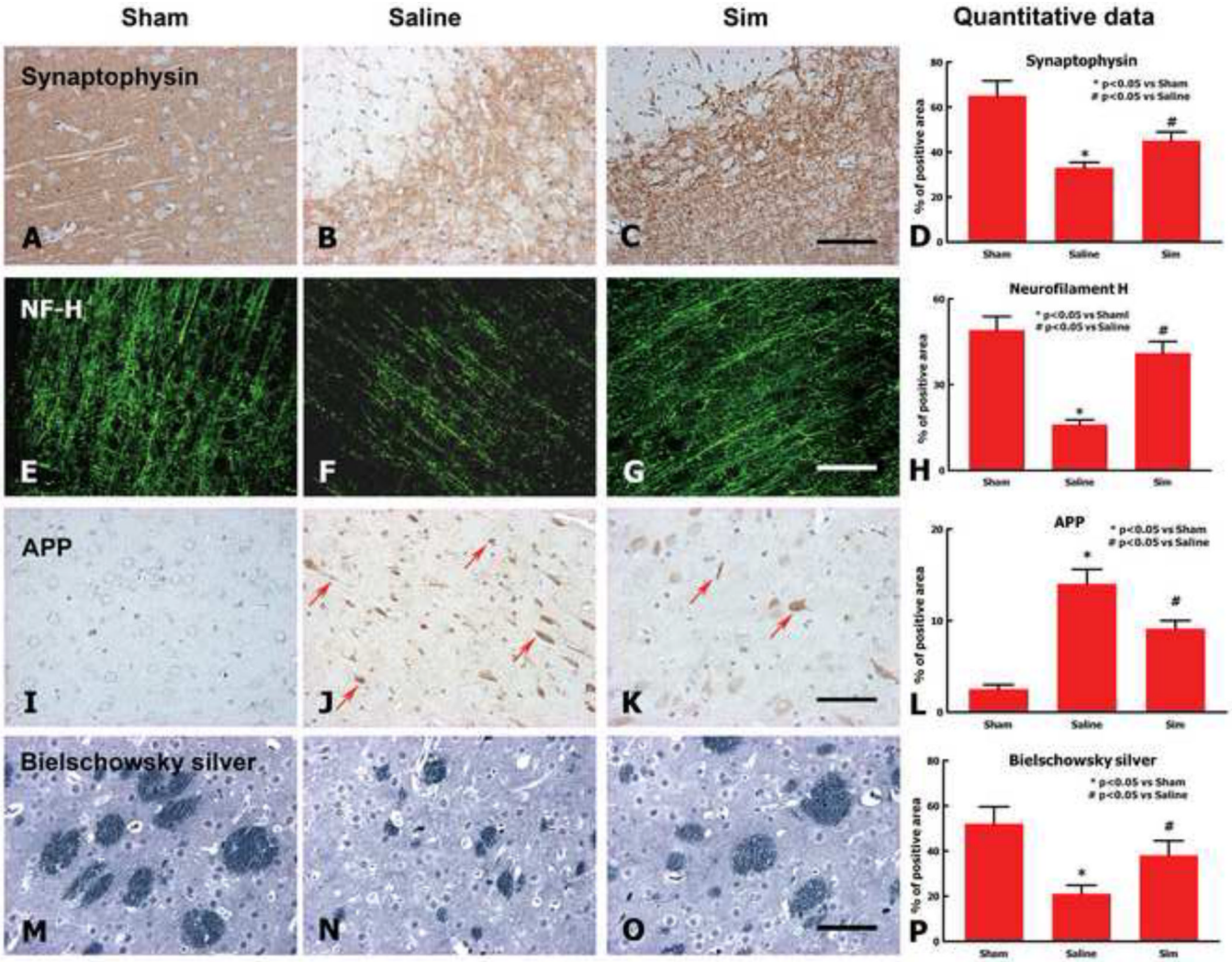

Fig. 2.

Photomicrographs showing the effect of simvastatin on axonal injury in the ipsilateral hemisphere 14 days after TBI. Treatment with simvastatin significantly increases synaptic density compared with saline control group (A-D). Simvastatin increases the axonal density (E-H & M-P) and reduces the density of APP-positive axons (I-L) compared with the saline-treated group. Data represent mean ± SD. The scale bars = 50 m (for all panels). n = 8/ group.

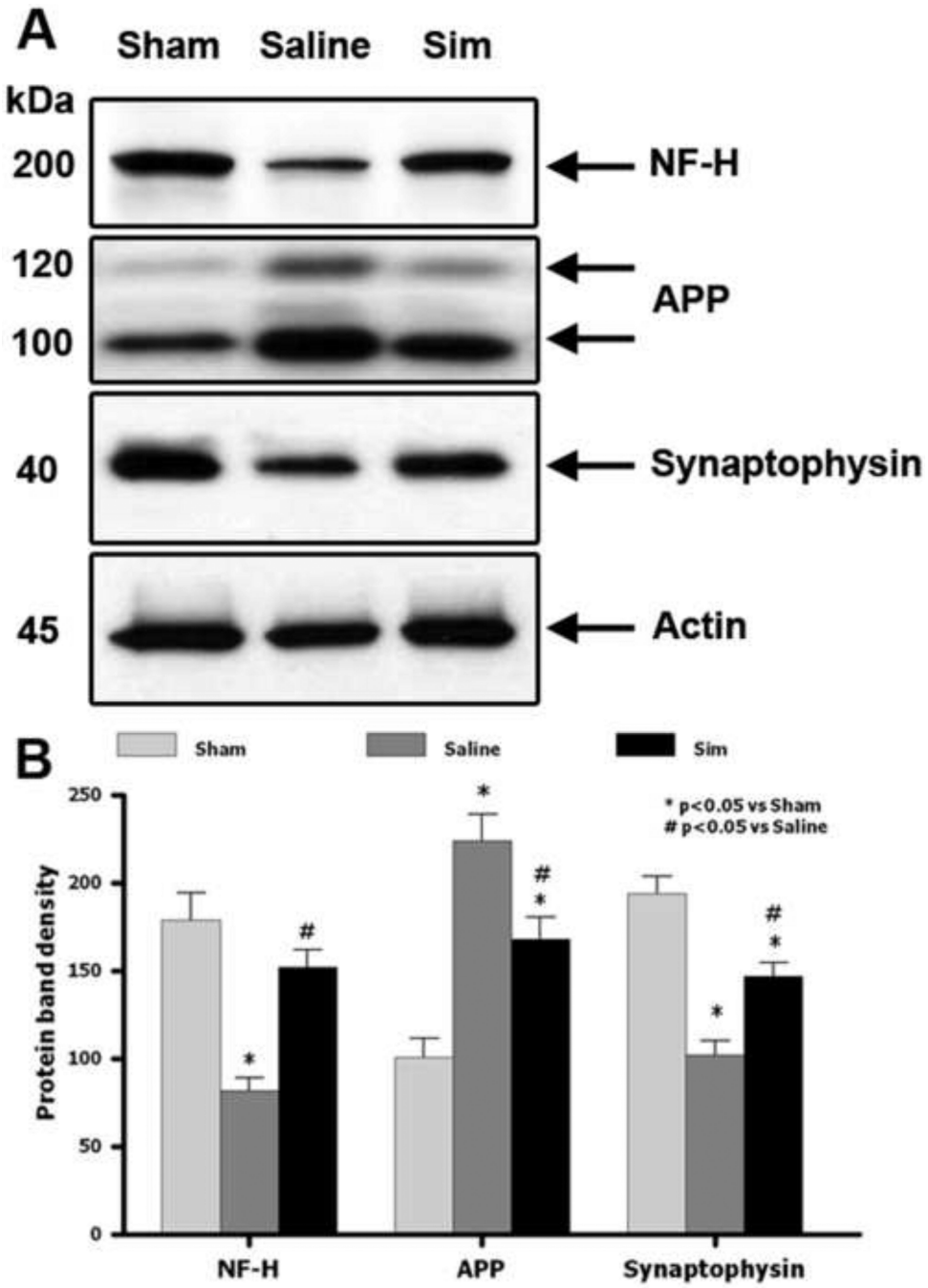

Fig. 3.

Representative Western blot (A) and densitometry measurement (B) of NF-H, APP and synaptophysin in the lesion boundary zone 14 days after TBI. Simvastatin reduces APP expression and increases the level of NF-H and synaptophysin in the ipsilateral cortex. Data in the bar graphs are represented as mean ± SD. **P* < 0.05 vs sham. # *P* < 0.05 vs saline. n = 4/group.

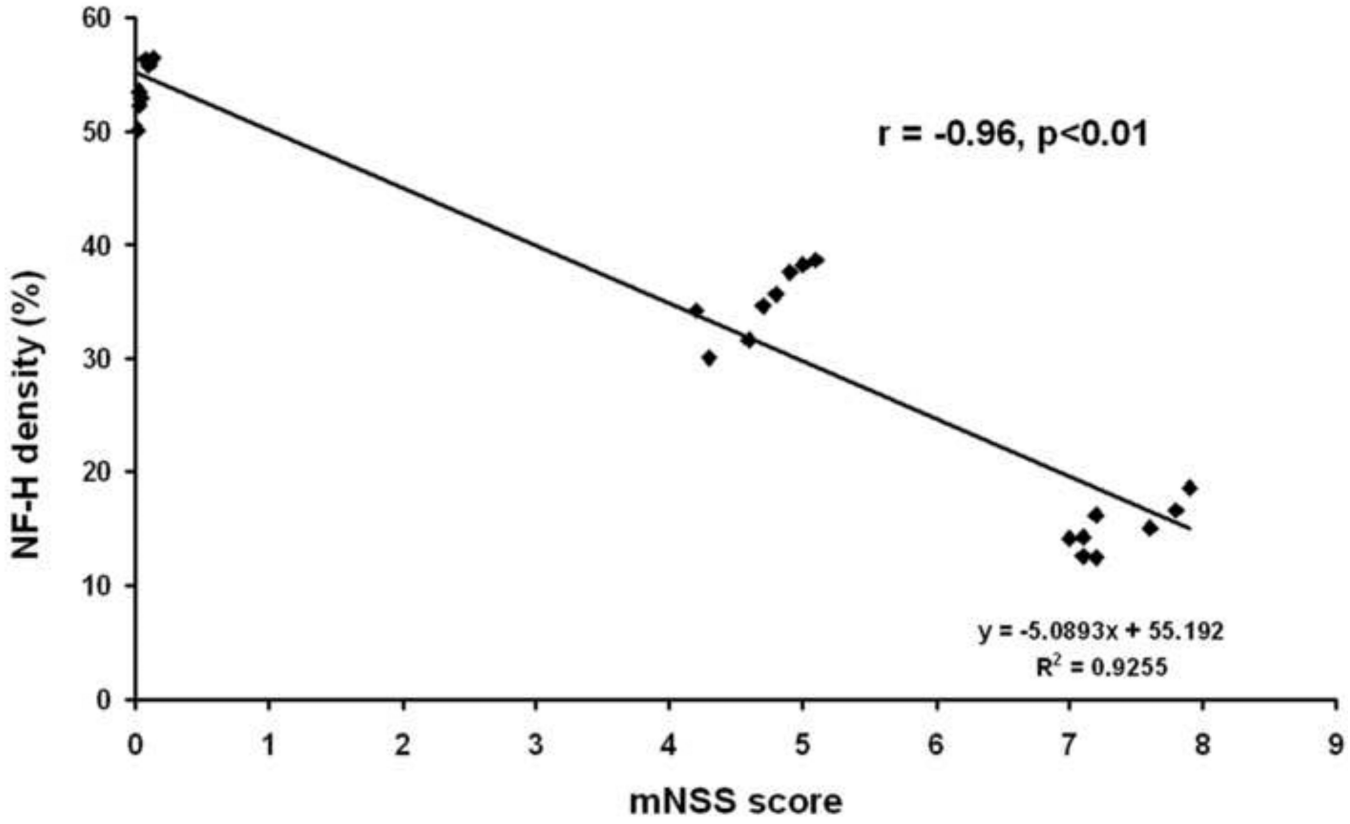

Fig. 4.

Correlation of sensorimotor functional recovery with the density of axons in the ipsilateral hemisphere. The graph shows that the score of mNSS is significantly and inversely correlated with the density of axons in the ipsilateral hemisphere at day 14 after TBI ($P < 0.01$). n = 8/group.

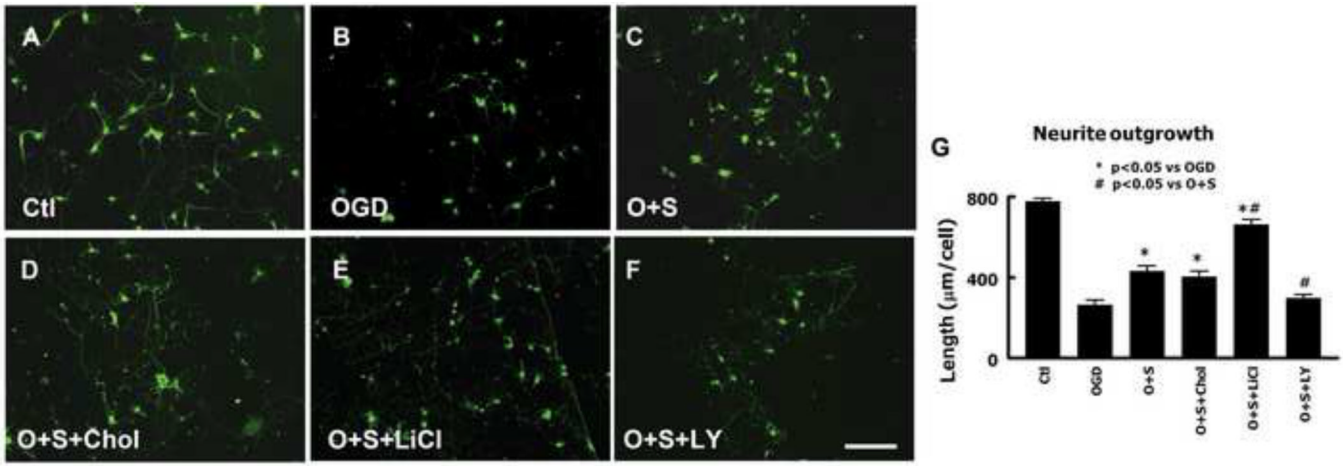

Fig. 5.

Immunofluorescent staining for TUJ-1 demonstrates neurite outgrowth of primary cultured cortical neurons *in vitro* under various treatments (A-F). Bar = 100 μm (for all panels). G: Bar graph showing the quantitative analysis of length of neurite outgrowth in variously treated groups, * $P < 0.05$ vs OGD, # $P < 0.05$ vs O + S. n = 4/group.

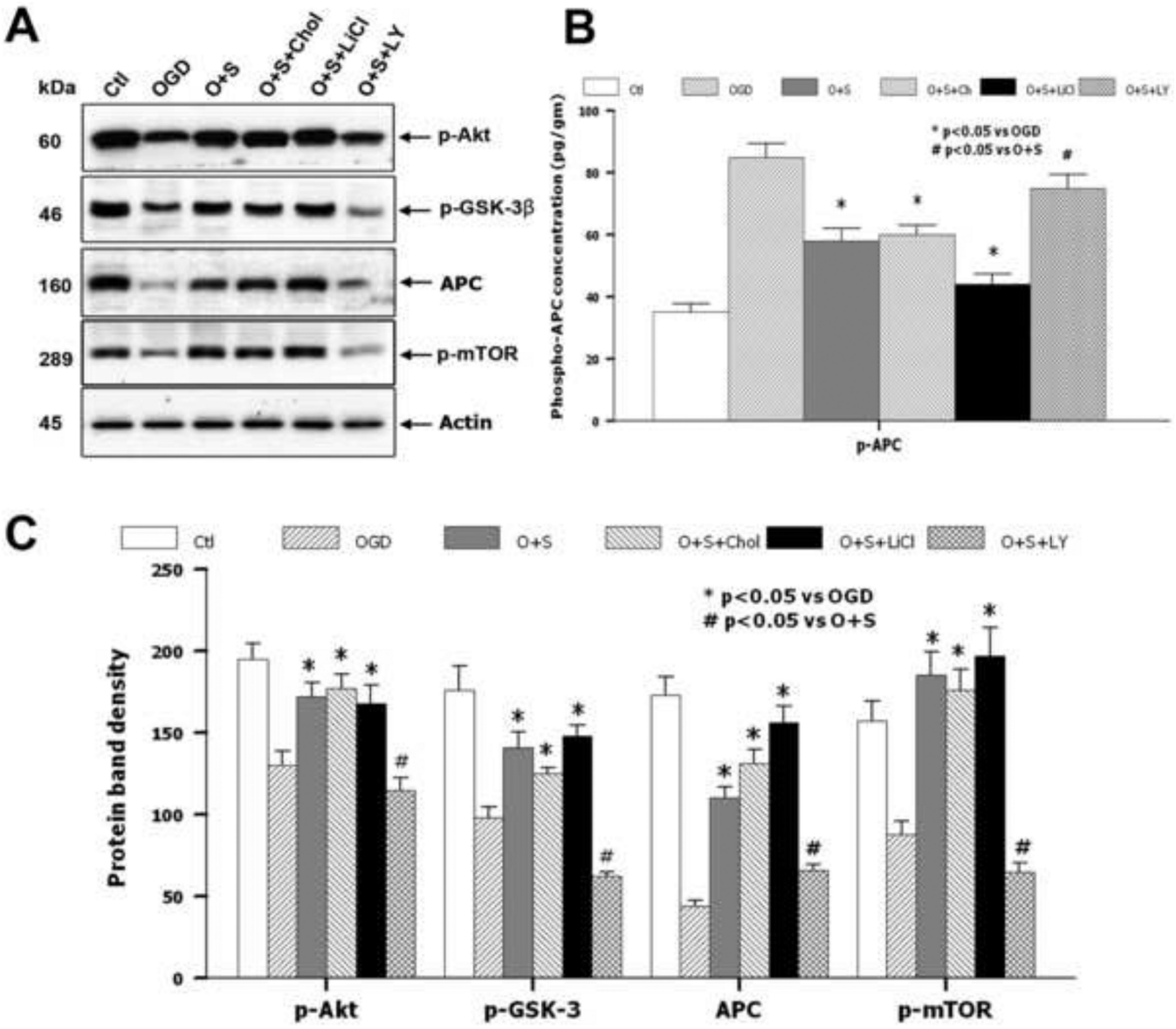

Fig. 6.

Representative Western blot (A) and densitometry measurement (B) of p-Akt, p-GSK-3β and APC in the cultured PCNs with various treatments after OGD. ELISA of p-APC levels in the PCNs with various treatments (C). Data in the bar graphs are represented as mean ± SD. *$P < 0.05$ vs OGD. # $P < 0.05$ vs O + S. n = 4/group.

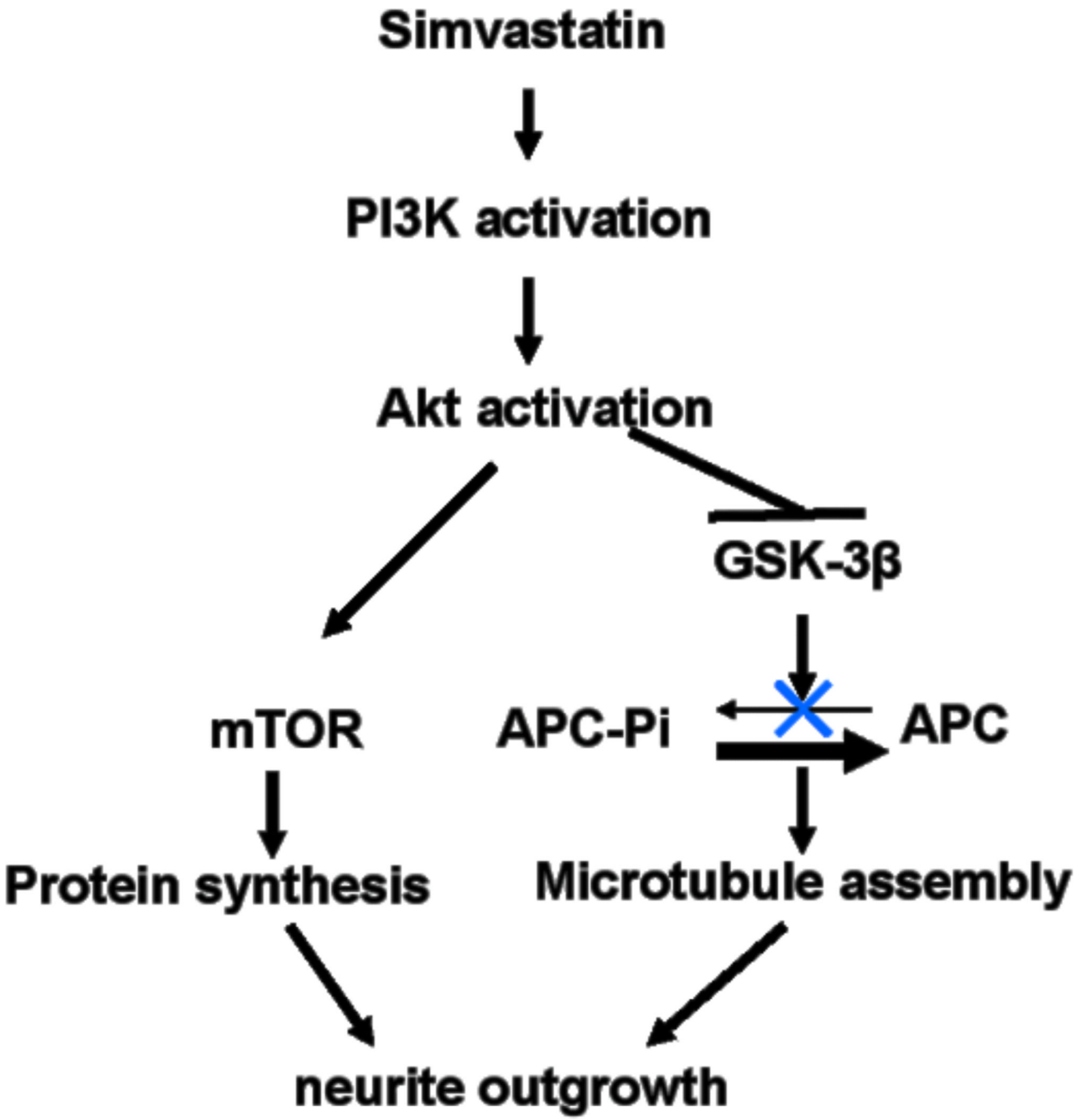

Fig. 7.

A proposed model for the signaling pathways mediating the effect of simvastatin on neurite outgrowth. Simvastatin activates PI-3K, which in turn phosphorylates and activates Akt. Akt controls a host of signaling molecules, including GSK-3β and mTOR. Activation of mTOR by Akt leads to increased protein translation and protein synthesis in the injured neurons. On the other hand, Akt phosphorylates and inactivates GSK-3β. Inactivation of GSK-3β dephosphorylates APC, facilitates APC binding to microtubules and eventually leads to microtubule assembly. Both the protein synthesis and the microtubule assembly contribute to the simvastatin-induced neurite outgrowth. '→' represents activation, ' ' represents inactivation, and 'x' represents blockage of APC phosphorylation.